Optimal Improvement of Post-Disturbance Dynamic Response in Power Grids

Mohamadsaleh Jafari, Mohammad Ashiqur Rahman, and Sumit Paudyal Department of Electrical and Computer Engineering, Florida International University, USA Emails: mjafa006@fiu.edu, marahman@fiu.edu, spaudyal@fiu.edu

Abstract—Any disturbance in power grids can lead to electromechanical oscillations leading to fluctuations in frequency and rotor angle of generators. If proper control actions are not taken, severe disturbances could lead to instability of the system. However, the dynamic response of the system depends on the set of control actions. Therefore, we propose to optimally enhance the dynamic response of multi-machine power systems following disturbances by controlling the reference set-point of the governors. To achieve this, we combine the famous DC power flow model of the grid with linearized dynamics of generators/governors to achieve scalable linear programming (LP) based optimization model that provides a set-point of the governors to achieve an optimal dynamic response of the generators. We validated the accuracy of the proposed models by comparing them with an off-the-shelf commercial dynamic modeling tool using the IEEE 39-bus test system. Thereafter, we use the proposed optimization model to dampen the frequency oscillations resulting from load disturbances. The results show that the proposed model can sufficiently capture the dynamic behavior of power grids and the comparison of frequency and rotor angle response obtained from the optimization-based approach show that the proposed method can greatly reduce the settling time of frequency and rotor angle responses compared to the non-optimized cases.

Index Terms—Power grid dynamics, Optimization, Oscillation dampening, DC power flow, Linear programming.

I. Nomenclature

Sets and Indices

| $\frac{a(.)}{dt}$ | Rate of change of a parameter. |
|-------------------|--------------------------------|
| n | Discrete step number. |
| $\mathcal G$ | Set of generator buses. |
| \mathcal{N} | Set of buses. |

U Set of generators equipped with governors.

 \mathcal{W} Set of discrete steps.

Parameters and Variables

| Generator's rotor angle. |
|---|
| Angular frequency. |
| Nominal angular frequency. |
| Angular frequency deviation from nominal. |
| Imaginary part of line admittance between bus i |
| and bus j . |
| Nominal frequency. |
| Synchronous generators' inertia constant. |
| |

D Load damping factor.

This work is supported in part by National Science Foundation grant ECCS-2001732, and FIU Graduate School Dissertation Year Fellowship (DYF).

| P^G | Generator's electrical power output. |
|---------------------|--|
| P^L | Load active power. |
| P^M | Generator's mechanical power input. |
| \overline{P}^M | The upper limit of generator mechanical power. |
| \underline{P}^{M} | Lower limit of generator mechanical power. |
| P^r | Governor's reference set-point. |
| R | Governors' speed droop. |
| T | Governors' time constant. |
| T^s | Discretization time-step size. |

II. INTRODUCTION

Electromechanical oscillations are unavoidable in power grids [1]. Any disturbance in power grids leads to electromechanical oscillations that cause fluctuations in frequency and rotor angle of generators, which can be captured using the dynamic models [2]. The set of control actions, such as governors' reference set points, determine how the dynamics evolve after the disturbances. Setpoints are updated every 2 to 4 seconds to regulate frequency in power grids [3], [4]. Hence, carefully and dynamically setting governors' reference set-points can enhance the overall dynamic response of power grids. Moreover, the reference setpoints could be designed optimally to enhance the dynamic response of the power grids, which is the main motivation behind the proposed work.

On the optimization side of the problem in power systems, optimal power flow (OPF) has been developed as a core tool in determining the optimal setpoint of the generators [5]. However, OPF conventionally only looked at the algebraic model of the grid; hence, it does not capture the dynamic response. Recently, OPF has been combined with additional constraints to enhance the stability of power grids [6]. In [7], the authors proposed an OPF method in which the loads' reactive power is controlled to dampen the oscillations. Reference [8] introduces a stability-constrained OPF to determine an operating point in transiently secure power grids. Similarly, [9] presents a global transient stability-constrained OPF. However, the proposed methods in [8], [9] only guarantee a new stable operating point that is stable but does not necessarily provide fast damping of oscillations. The scope of this proposed work looks at the optimal damping of system-level dynamics employing optimal dynamic setpoints of governors.

Dynamic modeling of power grids requires non-linear differential equations [10] and combining the dynamic models to OPF makes the problem inherently non-convex. To this end, we propose to adopt linearized grid dynamics (based on the Backward Euler method [11]) combined with the famous DC power flow-based grid model that yields linear programming (LP) formulation and hence ensures scalability.

The rest of the paper is organized as follows: In Section III, we present the continuous and discretized versions of power grid dynamic models. In Section IV, we introduce the proposed optimization model. Case studies are presented in Section V. We conclude the paper in Section VI.

III. DYNAMIC MODEL

A. Power System Dynamics

We adopt the classical representation of synchronous generators along with DC power flow. These modeling approaches are commonly utilized in the literature [12], [13]. Dynamic behavior of synchronous generators can be represented using the Swing equation as [4],

$$\frac{d\delta_i}{dt} = \omega_i - \omega_o = \Delta\omega_i, \quad \forall i \in \mathcal{N}, \quad (1)$$

$$\frac{d\omega_i}{dt} = \frac{1}{2H_i} \left(P_i^M - P_i^G - D_i \, \Delta\omega_i \right), \quad \forall i \in \mathcal{G}, \quad (2)$$

All the notations used in the formulations are provided in Section I. For brevity, we dropped the time index. We consider the classical representation of synchronous generators in which generators' rotor angles are approximated by the terminal voltage angles. The governor model TGOV1 (shown in Fig. 1) is considered, which is a simplified representation of steam turbine governors as in [14], and can be modeled as,

$$P_i^M = \frac{1}{T_i} \int \left(\frac{P_i^r - \Delta \omega_i}{R_i} - P_i^M \right), \quad \forall i \in \mathcal{U},$$
 (3)

The power grid can be modeled using DC power flow formulations as [4],

$$P_i^G - P_i^L = \sum_{j \in \mathcal{N}} B_{i,j} \left(\delta_i - \delta_j \right), \quad \forall i \in \mathcal{N},$$
 (4)

Equations (1)-(4) represent the dynamic model of multimachine power grids. We consider that the control center dispatches the generators based on DC power flow (4), and sends the reference set-points P^r to governors as follows,

$$P_i^r = R_i P_i^G, \quad \forall i \in \mathcal{U}, \tag{5}$$

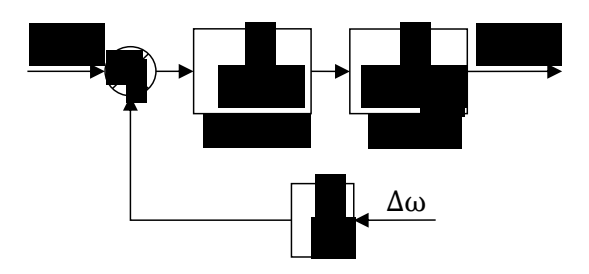


Fig. 1. TGOV1 model of governor

B. Discretized Dynamic Model

Using the Backward Euler method [11] to the dynamical model described in Section III.A, we obtain,

$$P_i^M[n+1] = P_i^M[n] + \frac{T^s}{R_i T_i} \left(P_i^r[n+1] - \Delta \omega_i[n+1] - R_i P_i^M[n+1] \right), \quad \forall i \in \mathcal{U}, \, \forall n \in \mathcal{W}, \quad (6)$$

$$\delta_{i}[n+1] = \delta_{i}[n] + T^{s} \Delta \omega_{i}[n+1], \forall i \in \mathcal{N}, \forall n \in \mathcal{W}, \quad (7)$$

$$\omega_{i}[n+1] = \omega_{i}[n] + \frac{T^{s}}{2H_{i}} \left(P_{i}^{M}[n+1] - P_{i}^{G}[n+1] - P_{i$$

$$D_i \Delta \omega_i[n+1]$$
, $\forall i \in \mathcal{G}, \forall n \in \mathcal{W}$, (8)

$$P_i^G[n] - P_i^L[n] = \sum_{j \in \mathcal{N}} B_{i,j} \left(\delta_i[n] - \delta_j[n] \right),$$

$$\forall i \in \mathcal{N}, \, \forall n \in \mathcal{W}, \quad (9)$$

$$P_i^r[n] = R_i P_i^G[n], \quad \forall i \in \mathcal{U}, \forall n \in \mathcal{W}.$$
 (10)

where (6) represents the generator's mechanical power input dynamics. Equations (7) and (8) model the dynamics of generators rotor angle and frequency, respectively. Equation (9) represents the DC power flow. Equation (10) relates the governors' reference set-points and generators' output. The resulting discretized dynamic model is linear in nature.

IV. OPTIMIZATION WITH GRID DYNAMICS

We aim at minimizing frequency oscillations in power grids by finding optimal setpoints of governors, which can be modeled as,

$$\mathbf{Min:} \quad \sum_{\substack{n \in \mathcal{W} \\ i \in G}} |\omega_i[n] - \omega_0|, \tag{11}$$

Equation (11) can be reformulated as an LP model. Next, we introduce optimization-based power grid dynamics modeling to find optimal values for P^r minimizing frequency oscillations in power grids. We combine the classical DC-OPF formulation and the discredited dynamic model discussed in Section III-B (referred to as the OPF-D model). The proposed OPF-D (12) aims at minimizing the frequency deviations from the nominal value. Moreover, considering the AC power flow makes an optimization problem non-convex in nature, therefore, we employ DC power flow in our proposed method and formulate the OPF-D as follows to make the overall problem LP which yields a tractable formulation.

OPF-D: Min:
$$\sum_{\substack{n \in \mathcal{W} \\ i \in G}} \Delta \omega_i[n]$$
 (12)

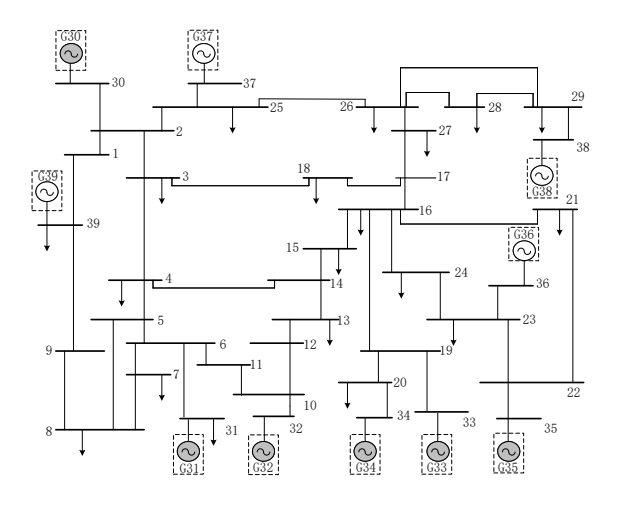
S. t.: Constraints (6) - (10),

$$\underline{P}_{i}^{M} \le P_{i}^{M}[n] \le \overline{P}_{i}^{M}, \quad \forall i \in \mathcal{U}, \forall n \in \mathcal{W}, \tag{13}$$

$$\Delta\omega_i[n] \ge \omega_i[n] - \omega_0, \quad \forall i \in \mathcal{G}, \forall n \in \mathcal{W},$$
 (14)

$$\Delta\omega_i[n] \ge \omega_0 - \omega_i[n], \quad \forall i \in \mathcal{G}, \forall n \in \mathcal{W},$$
 (15)

where (6)-(10) model the dynamics of power grids. Constraint (13) maintains the mechanical power input of generators



Generator eqquiped with governor
 Generator without governor

Fig. 2. IEEE 39-bus power system [4].

within the permissible range. Constraints (14) and (15) ensures the frequency around the nominal value, and is part of LP reformulation of (11). For simplicity, we didn't show the modeling of limitations such as transmission lines' overloading. However, such constraints can be readily included without changing the nature of the model.

V. NUMERICAL STUDIES

A. Test System

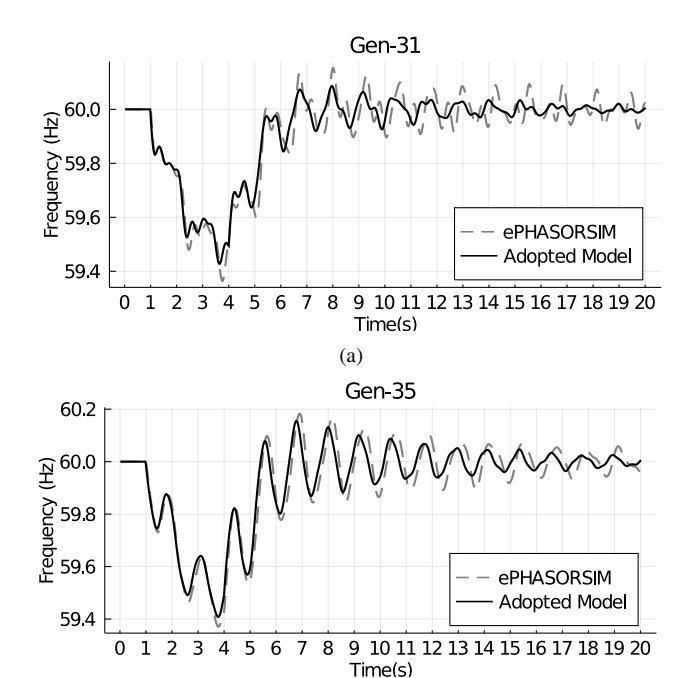
We use the IEEE 39-bus system as shown in Fig. 2 as the test system [4]. This system includes 10 synchronous generators with rated capacities of 1,000 MVA. It is assumed that the generators connected to buses 30 through 35 are equipped with governors, while the generators at buses 36 through 39 do not have any governors, i.e., the mechanical power input of these generators is fixed. The generators and governors' parameters are provided in Table I. Load damping factors are ignored, i.e., D=0, and bus 39 is considered the slack bus.

B. Model Validation

To validate the accuracy of the adopted dynamic model, we apply a load disturbance to the test system and compare the resulting dynamics with the solution obtained from ePHA-SORSIM. A discretization time-step of 0.016 s is used.

TABLE I
GENERATOR AND GOVERNOR PARAMETERS

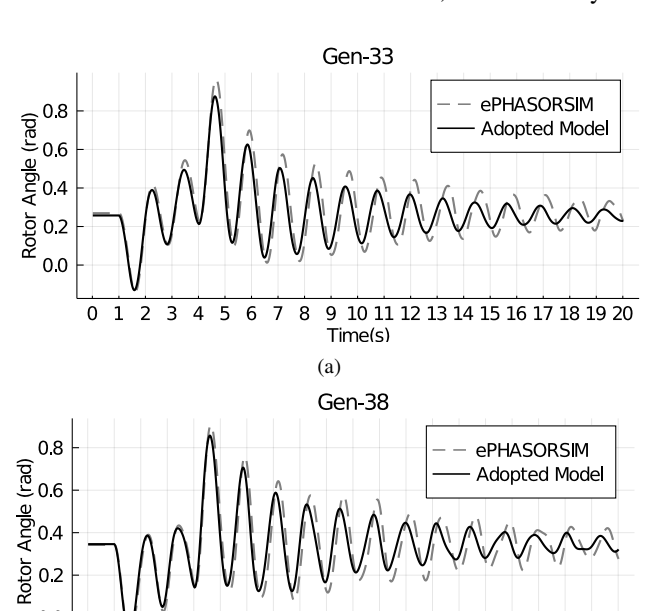
| Bus No. | Generator | Governor | |
|---------|-----------|----------|------|
| | H(s) | R(p.u.) | T(s) |
| 30 | 4.20 | 0.05 | 0.50 |
| 31 | 3.03 | 0.05 | 0.50 |
| 32 | 3.58 | 0.05 | 0.50 |
| 33 | 2.86 | 0.05 | 0.50 |
| 34 | 2.60 | 0.05 | 0.50 |
| 35 | 3.48 | 0.05 | 0.50 |
| 36 | 2.64 | - | - |
| 37 | 2.43 | - | - |
| 38 | 3.45 | - | - |
| 39 | 50.00 | - | - |



(b) Fig. 3. Frequency dynamics comparison of generators 31 and 35 between the proposed modeling and the simulation.

A load increase of 1,000 MW (50 MW at each load bus and equivalent to 16% of the total load) is applied for 3 s (beginning at $t=1\,\mathrm{s}$ and ending at $t=4\,\mathrm{s}$) on top of a base load of 6,150 MW. Fig. 3 shows the frequency dynamics of the select generators obtained from the adopted dynamic model and ePHASORSIM. Similarly, the dynamics of rotor angles of select generators are compared in Fig. 4.

From the figures, we can see that the dynamic responses are very close. The observed little discrepancy is mainly due to the use of AC power flow-based grid models in off-the-shelf commercial ePHASORSIM solver, while our dynamic



(b) Fig. 4. Comparison of the generators' 33 and 38 rotor angle behavior between the proposed modeling and the simulation.

9 10 11 12 13 14 15 16 17 18 19 20

0.0

4 5 6 7 8

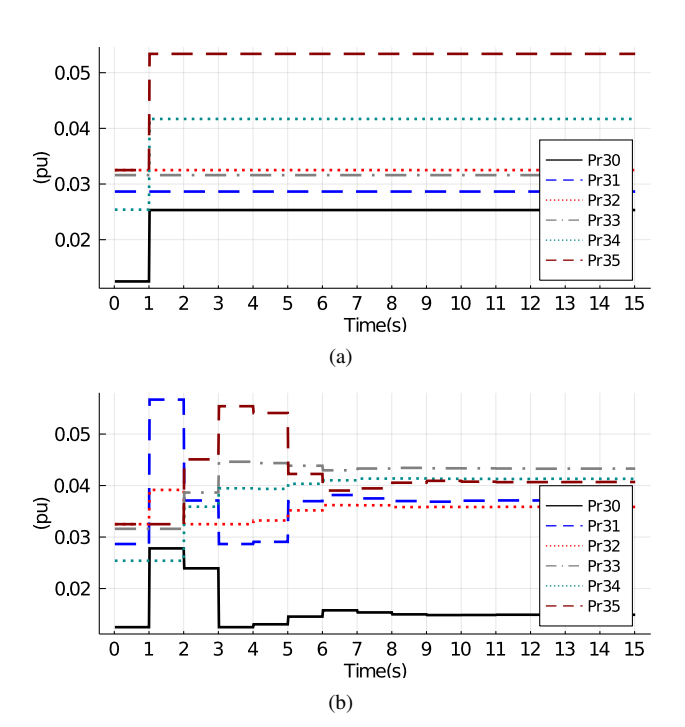


Fig. 5. Comparison of non-optimal governors' reference set-points and optimal ones from the proposed OPF-D.

model is based on the DC power flow-based grid model. The main motivation to use the DC power flow-based grid model in this work is to keep the resulting optimization model linear in nature which ensures scalability.

C. Optimal Dynamic Response

In this part, we aim at showing the performance of the proposed OPF-D in minimizing the oscillations in power grids after disturbances. The proposed OPF-D in this paper is implemented in JuMP [15] and is solved using Gurobi [16]. As mentioned before, OPF-D gives the optimal P^r for governors so that the oscillations are dampened as fast as possible. To this end, we consider the same load disturbance as Section V-B which lasts for 15 s (starting at t = 1 s and ending at $t = 15 \,\mathrm{s}$), and study two scenarios of setting governors' reference sepoints, i.e., optimal and non-optimal, as shown in Fig. 5. Fig. 5(a) shows a non-optimal dispatch of generators where the power balance is ensured but did not care about the dynamic response. Since the load disturbance is constant after its incident at t = 1 s, therefore, P^r s are updated only once in non-optimized case. On the other hand, Fig. 5(b) demonstrates the optimal dispatch of the proposed OPF-D for the same load disturbance. Although the load changes only once, P^r s are dynamically and optimally updated to minimize the oscillations.

The comparison of the performance of OPF-D versus the non-optimal dispatch scenario is shown in Fig. 6 and 7. Fig. 6 shows this comparison for the frequency behavior of the 10 generators in the test system, and Fig. 7 shows the rotor angles' behavior of those generators. Note that all the rotor angles are relative to the slack bus generator's rotor angle. Therefore, we do not show any plot for the rotor angle of the slack bus generator. These figures clearly demonstrate the

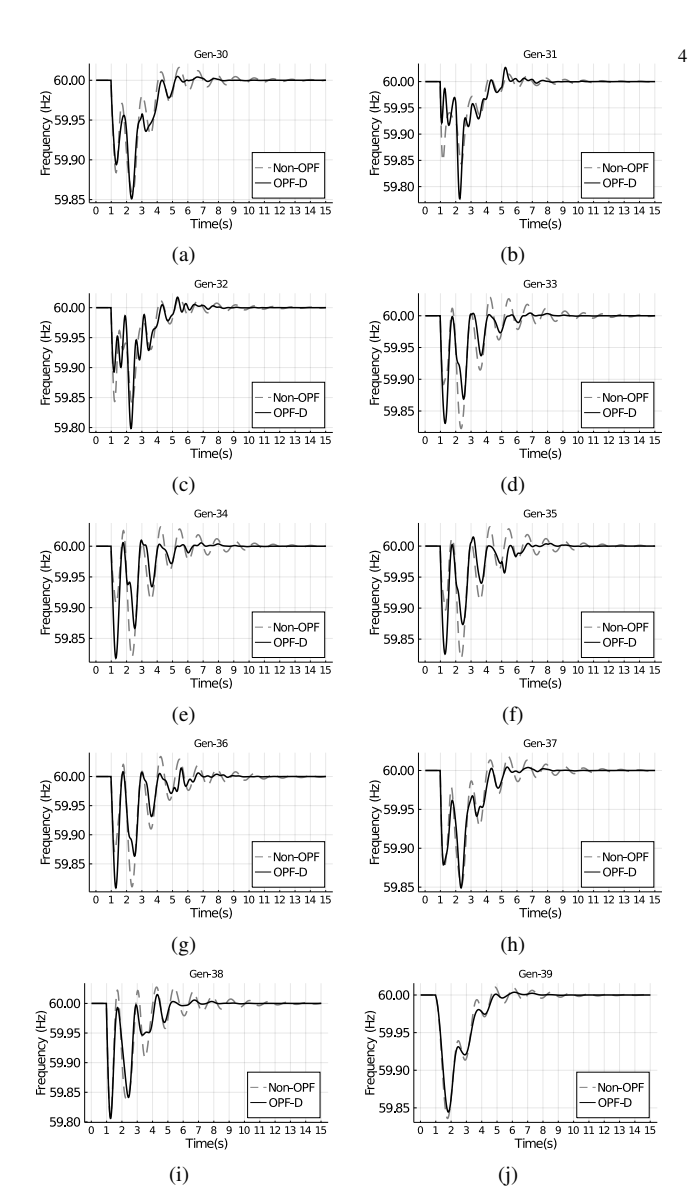


Fig. 6. Demonstration of generators' frequency dynamics for optimal and non-optimal dispatch.

ability of the proposed OPF-D in dampening the oscillations fast in the test system. The reason for some large oscillations in the optimal case is that the ramp limit on the frequency and upper bounds on the frequency are not enforced. The comparison of the settling time of the generators' frequencies and rotor angles is also provided in Table II and III. We define the frequency settling time as the time when the frequency stays within \pm 0.06 Hz of the nominal value i.e., [59.94,60.06] Hz. Similarly, the settling time for the rotor angle dynamics is defined as the time when the oscillations stay within \pm 1% of their corresponding steady-state values.

It can be seen that the settling times of the cases corresponding to optimal P^r s derived by the proposed OPF-D are enhanced, which ensures lower frequency and rotor angle oscillations compared to the non-optimized cases. For one generator (G39) the damping was worsen compared to the base case as the objective function (12) tries to improve the frequency response cumulative of all generators, rather not of a single generator.

VI. CONCLUSION

In this paper, we modeled power grid dynamics in an optimization environment. We modeled the classical represen-

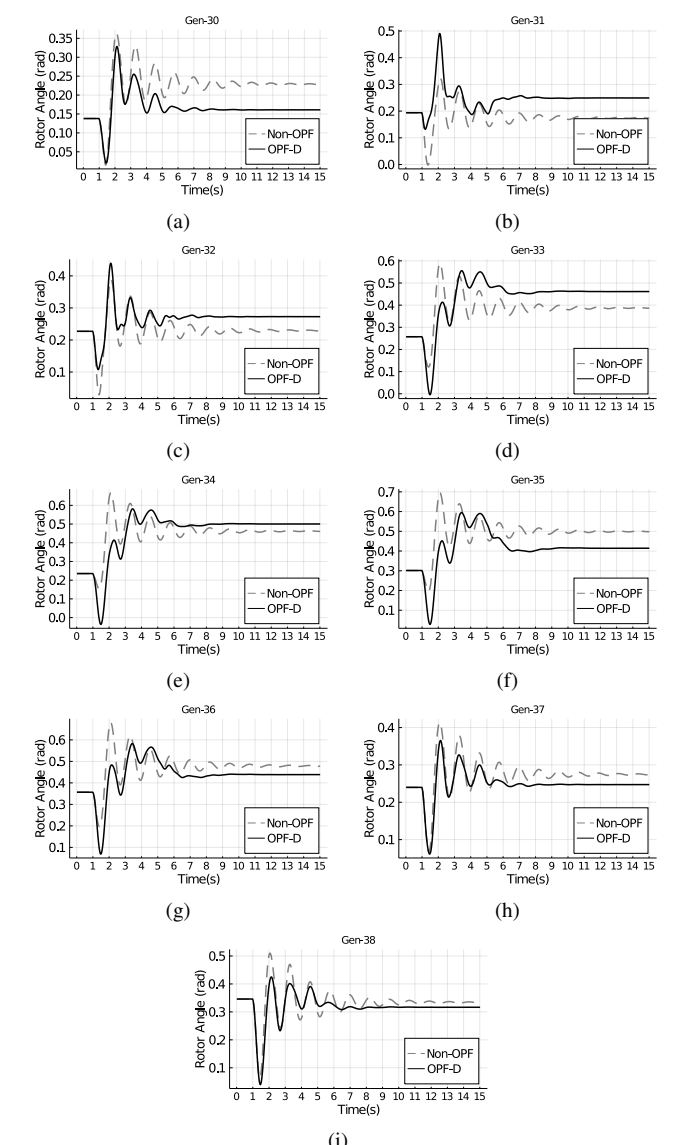


Fig. 7. Demonstration of generators' rotor angle dynamics for optimal and non-optimal dispatch.

TABLE II SETTLING TIME OF GENERATORS' FREQUENCY (IN SECOND).

| | | | ()- |
|---------|----------------------|------------------|-------------|
| Gen No. | Settling time | Settling time | Improvement |
| | (Non-optimal P^r) | (Optimal P^r) | improvement |
| 30 | 3.767 | 3.700 | -0.067 |
| 31 | 3.767 | 3.683 | -0.084 |
| 32 | 3.783 | 3.617 | -0.166 |
| 33 | 3.850 | 3.800 | -0.050 |
| 34 | 3.850 | 3.800 | -0.050 |
| 35 | 3.850 | 3.800 | -0.050 |
| 36 | 3.850 | 3.800 | -0.050 |
| 37 | 3.767 | 3.517 | -0.250 |
| 38 | 3.783 | 3.517 | -0.266 |
| 39 | 3.283 | 3.217 | 0.034 |
| | | | |

tation of synchronous generators and the TGOV1 model for governors along with DC power flow. Employing the Backward Euler method and converting the continuous equations to discretized, we proposed OPF-D to minimize the frequency deviations in power grids by optimally and dynamically setting the reference set-points to governors. We validated the dynamic model using the ePHASORIM solver for the IEEE 39 bus system developed. Thereafter, we studied case studies to compare settling times of the generators' frequencies and

TABLE III
SETTLING TIME OF ROTOR ANGELS (IN SECOND).

| Gen No. | Settling time (Non-optimal P^r) | Settling time (Optimal P^r) | Improvement |
|---------|------------------------------------|--------------------------------|-------------|
| 30 | 8.350 | 4.883 | -3.467 |
| 31 | 8.333 | 5.467 | -2.866 |
| 32 | 8.850 | 5.350 | -3.500 |
| 33 | 9.550 | 6.733 | -2.817 |
| 34 | 9.550 | 6.850 | -2.700 |
| 35 | 9.550 | 8.083 | -1.467 |
| 36 | 9.567 | 7.883 | -1.684 |
| 37 | 8.883 | 5.833 | -3.050 |
| 38 | 9.550 | 5.967 | -3.583 |

rotor angles. The results clarify that our proposed OPF-D is able to greatly capture the detail of power grids' dynamics and reduce the damping time of frequency oscillation. In future work, we will model a detailed representation of synchronous generators e.g., the sixth-order, along with excitation systems, and power grid stabilizers. Moreover, we will consider the secondary frequency control in governors' behavior modeling as well and show the scalability of the model in a large-scale power grid.

REFERENCES

- B. M. Weedy, B. J. Cory, N. Jenkins, J. B. Ekanayake, and G. Strbac, *Electric Power Systems*. John Wiley & Sons, 2012.
- [2] G. Andersson, "Modelling and analysis of electric power systems," EEH-Power Systems Laboratory, Swiss Federal Institute of Technology (ETH), Zürich, Switzerland, 2008.
- [3] R. Shankar, S. Pradhan, K. Chatterjee, and R. Mandal, "A comprehensive state of the art literature survey on LFC mechanism for power system," *Renewable and Sustain. Energy Reviews*, vol. 76, pp. 1185–1207, 2017.
- [4] P. Kundur, Power System Stability. CRC Press New York, NY, USA, 2007, vol. 10.
- [5] M. Huneault and F. D. Galiana, "A survey of the optimal power flow literature," *IEEE Tran. Power Syst.*, vol. 6, no. 2, pp. 762–770, 1991.
- [6] S. Abhyankar, G. Geng, M. Anitescu, X. Wang, and V. Dinavahi, "Solution techniques for transient stability-constrained optimal power flow-Part I," *IET Generation, Transmission & Distribution*, vol. 11, no. 12, pp. 3177–3185, 2017.
- [7] M. Inoue, T. Sadamoto, M. Arahata, and A. Chakrabortty, "Optimal power flow design for enhancing dynamic performance: Potentials of reactive power," *IEEE Tran. on Smart Grid*, vol. 12, no. 1, pp. 599– 611, 2020.
- [8] D. Gan, R. J. Thomas, and R. D. Zimmerman, "Stability-constrained optimal power flow," *IEEE Tran. Power Syst.*, vol. 15, no. 2, pp. 535– 540, 2000.
- [9] A. Pizano-Martinez, C. R. Fuerte-Esquivel, and D. Ruiz-Vega, "A new practical approach to transient stability-constrained optimal power flow," *IEEE Tran. Power Syst.*, vol. 26, no. 3, pp. 1686–1696, 2011.
- [10] J. Das, Load Flow Optimization and Optimal Power Flow. CRC Press,
- [11] B. P. Zeigler, A. Muzy, and E. Kofman, Theory of modeling and simulation: Discrete event & iterative system computational foundations. Academic press, 2018.
- [12] X. Zhao, H. Wei, J. Qi, P. Li, and X. Bai, "Frequency stability constrained optimal power flow incorporating differential algebraic equations of governor dynamics," *IEEE Trans. Power Syst.*, vol. 36, no. 3, pp. 1666–1676, 2020.
- [13] S. Amini, F. Pasqualetti, and H. Mohsenian-Rad, "Dynamic load altering attacks against power system stability: Attack models and protection schemes," *IEEE Trans. Smart Grid*, vol. 9, no. 4, pp. 2862–2872, 2016.
- [14] I. C. Report, "Dynamic models for steam and hydro turbines in power system studies," *IEEE Trans. Power App. and Sys.*, vol. PAS-92, no. 6, pp. 1904–1915, 1973.
- [15] I. Dunning, J. Huchette, and M. Lubin, "JuMP: A modeling language for mathematical optimization," SIAM Review, vol. 59, no. 2, pp. 295–320, 2017
- [16] Gurobi Optimization, LLC, "Gurobi optimizer reference manual," 2022. [Online]. Available: https://www.gurobi.com